

Article ID: 1006-8775(2005) 02-0187-13

## IMPACT STUDY ON THE CALCULATION OF VERTICAL VELOCITY IN DIFFERENT VERTICAL COORDINATE SYSTEMS

LI Xing-liang (李兴良), CHEN De-hui (陈德辉), SHEN Xue-shun(沈学顺)

(Chinese Academy of Meteorological Sciences, Beijing 100081 China)

**ABSTRACT:** With the development of high-resolution and multi-scale unified numerical model, some of techniques about non-hydrostatic meso-scale numerical weather prediction are addressed. The impact of the vertical coordinate system is one of them. In this paper, based on a WRF (Weather Research and Forecast) model, the impact on the calculation of vertical velocity was studied with different vertical coordinates. The simulation results showed that the calculation of vertical velocity is sensitive to vertical coordinates. It is especially more evident when the resolution increased. Due to the close relationships between vertical velocity and precipitation, the difference of vertical velocity inevitably influences model's description of precipitation. An ideal experiment exhibits that pressure gradient force computations in the pressure terrain-following coordinate are sensitive to surface pressure.

**Key words:** numerical prediction models; coordinate system; vertical velocity; pressure gradient force

**CLC number:** P435.1      **Document code:** A

### 1 INTRODUCTION

First, let's have a review of various vertical coordinate systems used in numerical weather prediction (NWP). Richardson<sup>[1]</sup> (1922) first attempted to use the geometrical height  $z$  as the vertical coordinate system. Though geometrical height is easy to understand as a concept, it had not been applied in NWP until Kasahara and Washington (1967) rewrote his predictive equations and used state-of-the-art high-speed computers to conduct NWP in height coordinates. Eliassen<sup>[2]</sup> (1949) was the first person to use pressure ( $p$ ) as the vertical coordinate and it had become popular in the 1950's. As shown by what Sutcliffe (1947) and Godart and Eliassen (1949) had done, theoretic analysis of large-scale motion is made easier, especially in quasi-geostrophic models, for the mass continuous equation has been reduced to a diagnostic one by taking the pressure coordinates as the vertical coordinates. Many models using pressure in the vertical coordinates were then formulated and run successfully. Though pressure coordinate systems have computational shortcomings just above topographic features, as the lower boundary of the atmosphere is not a plane of the coordinate system. Phillips<sup>[2]</sup> (1957) was the first to propose a so-called sigma coordinate system ( $\sigma = p/p_s$ ), which is the transformed pressure coordinates, whose planes are the earth's surface. As a result, the sigma coordinate system based on primitive

---

**Received date:** 2004-06-28; **revised date:** 2005-07-08

**Foundation item:** Innovative Research on the Techniques of Numerical Meteorological Forecasting Systems in China — a National Key Scientific and Technological Project for the 10<sup>th</sup> Five-year Economic Development Plan (2001BA607B02); Research on topographic effects by the Chinese Academy of Meteorological Sciences (7048/2002-9y-1)

**Biography:** LI Xing-liang (1977 –), male, native from Shaowu County Fujian Province, M.S., mainly undertaking the study of numerical weather prediction.

E-mail: [lixliang@126.com](mailto:lixliang@126.com)

predictive equations were used in many of the weather forecasting models in the 1960's. Then, Sangster<sup>[4]</sup> (1960) proposed the use of mixed coordinates as the vertical coordinates, which employs the sigma system at lower levels but replaces it with the  $p$ -coordinates at higher levels. It goes around small differences of two large terms in the pressure gradient force with higher-level momentum equations but still encounters insufficiencies with the sigma coordinates at lower levels. Schlesinger and Mintz (1979) and Fles et al. (1980) adopted this coordinate system. In the 1970's, it was popular for people to use potential temperature as the vertical coordinates in objective weather analysis. It is interesting that vertical coordinates with potential temperature seem to be more appropriate for frontal structure. In treating lower boundary condition with the  $\theta$  coordinates, however, problems as complicated as with isobaric coordinate system ( $p$ -coordinates) were met. Meanwhile, Gal-Chen and Sommerville<sup>[5]</sup> (1975) put forward a height-based, terrain-following coordinate and applied it in the Navier-Stocks equation. In the 1980's, Mesinger<sup>[6]</sup> (1984) proposed the  $\eta$ -coordinate system, which is an improved version of the  $\sigma$ -coordinate system and originated from Egger's topographic blocking method (1972). It was put forward to remove issues of substantial errors arising from computing horizontal pressure gradient force, tropopause and horizontal diffusion along steep topographic plane of the coordinates. The system is based on quasi-horizontal  $p$ -planes so that it obtains simpler solutions of the momentum equations. Though the  $\eta$ -coordinate system does not do well in retaining finer details of the vertical structure of the boundary layer or giving accurate description of continuous terrain, nor make good forecasts of the leeward wind over steep topography.

Viewing the change from earlier geometric height coordinate system to the  $\eta$ -coordinate system, we can conclude that present model designers are more willing to use the terrain-following coordinate system. They have several important advantages. First of all, the whole field of the atmosphere is projected accounting for the vertical coordinate system of the square computation, whose digital structure is right for digital computers. Second, with such coordinate system, vertical winds transformed in the computed space disappear at the topographic levels. The transformation simplifies the condition of lower boundaries. Last, as the method allows for unequal intervals of space on the layers derived, it is equivalent of offering a very simple way to couple the dynamics of atmospheric forecasting models and parameterization schemes for the boundary and surface levels. It should be, of course, worthwhile to note that the terrain-following coordinates have disadvantages of their own. Its inclusion changes the term of pressure gradient force to small differences of two large terms in the geometric height coordinates and may lead to computational errors of the pressure gradient force, especially at the steep sections of the terrain.

Traditional NWP models are usually based on hydrostatic balance. With the improvement of high-performance computers, the resolution of numerical prediction has been increasing and highlighting the role of non-hydrostatic processes. At present, there are two kinds of vertical coordinate systems widely used to construct the dynamic framework of non-hydrostatic NWP models. One is the pressure- and terrain-following coordinates, which, in Laprise's opinion<sup>[7]</sup> (1992), is based on fully compressible equations and the hydrostatic pressure coordinates can be used in non-hydrostatic NWP models, e.g. the WRF model. The other is the height-based and terrain-following coordinates, which was first put forward by Gal-Chen and Sommerville (1975) and a new-generation Global and Regional Assimilation and Prediction System (GRAPeS) developed by the China Meteorological Administration is one such example. For a non-static equilibrium model, few concerted efforts have been made to study what vertical coordinates can better describe vertical motion under the condition that the computation of vertical velocity is associated with vertical coordinates. When the mesoscale model resolutions increased (1000 m, 500 m, for instance), it is more necessary to do so. The current work deals with the effects of different vertical coordinates on the computation of vertical velocity.

The second section of this paper gives an account to the WRF model and vertical coordinates.

The third section involves itself in theoretic analysis of the two coordinates to find out their key differences and conducts theoretic experiments with pressure gradient force at places of steep topography. Based on the theoretic analysis in the last section, meaningful comparisons are made in the fourth section of an unusually heavy rainstorm in Xi'an and Hanzhong, Shanxi province that took place from 20:00 June 7 to 02:00 June 10 (Local Time). The fifth section concludes on the description given with the vertical structure of the two coordinates.

## 2 WRF MODEL AND VERTICAL COORDINATES

### 2.1 The WRF model

The WRF model is a new-generation mesoscale model, which was developed at the National Center for Atmospheric Research (NCAR), National Centers for Environmental Prediction, Forecast Systems Laboratory (FSL), National Oceanic & Atmospheric Administration (NOAA), Center for Analysis and Prediction of Storms (CAPS), National Aeronautics and Space Administration (NASA), Air Force Weather Agency (AFWA) and many other societies and universities that took part in the cooperation. The procedure of WRF is so designed that it can be transplanted, maintained, expanded, readable, usable, structurally operational and interchangeable, and it can be used repeatedly in limited-area models with boundary condition and nesting.

### 2.2 Differences of height and mass coordinates

The height-based and terrain-following coordinates (to be simplified as height coordinates) can be written as

$$s_z = Z_T \frac{Z - Z_s}{Z_T - Z_s} \quad (1)$$

while the pressure-based and terrain-following coordinates (to be simplified as mass coordinates) can be written as

$$s_p = \frac{p - p_t}{p_s - p_t} \quad (2)$$

When pressure gradient force in the geometric height coordinates is transformed to sigma terrain-following coordinates, the formula used is expressed as the following by Arira Kasahar, which takes the pressure gradient force as example:

$$\nabla_z p = \nabla_s p - \left(\frac{\partial s}{\partial z}\right)_z \cdot \nabla_s Z \cdot \frac{\partial p}{\partial s} \quad (3)$$

In the height and mass coordinates, the expressions are respectively displayed as

$$-a \nabla_z p = -a \nabla_{s_z} p - \frac{Z_t - s_z}{Z_t} \cdot \nabla_{s_z} f_s \quad (4)$$

$$-a \nabla_z p = -\nabla_p f = -\nabla_{s_p} f - \left(\frac{p - p_t}{p}\right) \cdot RT \cdot \nabla_{s_p} \ln(p_s - p_t) \quad (5)$$

where  $p$  is the component of hydrostatic pressure,  $p_s$  and  $p_t$  are the values of pressure along the land surface and upper boundary, and  $Z_s$  and  $Z_T$  are the topographic height and top of the upper boundary layer.

From Eqs.(4) and (5), it is known that, as shown in the introduction, the selection of the sigma terrain-following coordinates may change one term in the geometric height coordinates ( $Z$ ) or the pressure coordinates ( $p$ ) to two main terms during the computation of some physical quantities. The two terms are just opposite in sign and thus lead to small differences in two large

terms. It is more clearly shown in Tab.1.

Tab.1 Comparisons of metric terms of slope on coordinate planes between the  $s_z$  and  $s_p$  systems

	Height-based and terrain-following coordinates “ $s_z$ ”	Pressure-based and terrain-following coordinates “ $s_p$ ”
With terrain	Equivalent to height coordinates “ $Z$ ”	Not equivalent to height coordinates “ $p$ ”
Given gridpoints	Metric term as “constant” in hydrostatic condition	Metric term varying with time in hydrostatic condition
symbols	Symbols of the metric term fixed; negative for windward slope but positive for leeward slope	Symbols of the metric term not fixed; can be positive or negative anytime, anywhere
when $z \rightarrow Z_T$	The metric term tends to be zero; planes “ $s_z$ ” coordinates automatically tend to be horizontal	The metric term (absolute value) are decreasing but not closing in to zero

### 2.3 Relationship between vertical coordinates and terrain

In theory, it does not matter much as to what kind of vertical coordinates are selected so long as it satisfies the levels of mathematical and physical foundation, i.e. keeps monotonous consistency. Liao et al. made complete description and proof about it. The transformation of coordinates only change the form of the equation sets and boundary condition. For example, the equation of vertical motion

$$\frac{dw}{dt} = -\frac{1}{r} \frac{\partial p}{\partial z} + fu - g \quad (6)$$

in which  $W = 0$  when  $Z_T = 0$  (the upper boundary);  $W = V_H \cdot \nabla H$  when  $Z=H$  (the lower boundary).

When the terrain-following coordinate  $s = \frac{p - p_T}{m}$  is used, it is expressed as

$$\frac{\partial W}{\partial t} + (\nabla \cdot \vec{V} W)_s - g \left( \frac{\partial p}{\partial s} - m \right) = F_w, m = p_s - p_T \quad (7)$$

in which the upper and lower boundaries are  $\dot{s} = 0, s = 0, 1 (\dot{s} = \frac{ds}{dt})$ .

It is worth noting that the terrain-following coordinates is so selected that the change in boundary condition resulted from the transformation is directly linked with the terrain at the lower boundary. The terrain-following coordinates compared in this work — the height and mass coordinates are showing just that. When the height and mass coordinates are selected, the upper and lower boundaries are respectively taken as

$s_z = 0$  at  $Z=Z_s$ ;  $s_z = Z_i$  at  $Z=Z_i$  for the height coordinate;

$s_p = 1$  at  $p=p_s$ ;  $s_p = 0$  at  $p=p_T$  for the mass coordinate.

The above analysis shows that the selection of coordinates in NWP models directly associates with the evaluation of both the upper and lower boundaries, with the lowest model layer being terrain surface. It is then seen that the lowest model surface during model prediction reflects true model terrain. In this way, the coordinates are directly linked with the terrain<sup>[7]</sup>. The slope of the model terrain given in Fig.1 is just that of the lower boundary.

## 3 IDEAL EXPERIMENT WITH SENSITIVITY OF COMPUTATION OF SURFACE PRESSURE

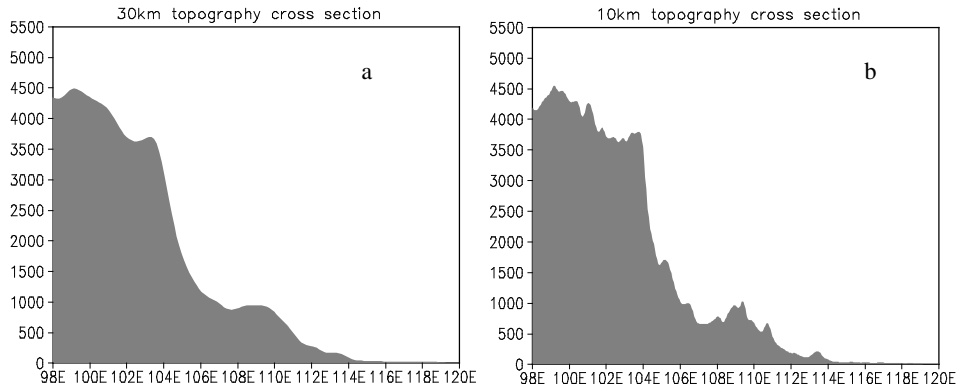


Fig.1 Comparisons of terrain slope obtained with the model along 33°N with resolution at 30 km (a) and 10 km (b), respectively.

### 3.1 Theoretic analysis of the computation of pressure gradient force with different vertical coordinates

It is well known that it is very convenient to process the upper and lower model boundaries with pure mathematical transformation of the Cartesian geometric height coordinates to the sigma coordinates. For instance, as the plane of the sigma coordinates is that of the underlying surface, the component of vertical velocity on the former becomes zero naturally, skipping the problem of determining the component of vertical velocity in the geometric height coordinates. It is, however, accompanied with some trouble with the computation of some physical quantities, errors at places where there is steep terrain in particular, and the derivation of pressure gradient force is one of them.

Studying Eqs.(4) and (5), we note that a main difference of computation of the pressure gradient force between the two coordinates lies in the difference of coordinate slope, i.e. the computation of  $\left(\frac{\partial s}{\partial z}\right)_z$ . It is clear that the computation of single-site pressure gradient for terrain slope with the height-based and terrain-following coordinate,  $\frac{Z_t - s_z}{Z_t} \cdot \nabla_{s_z} f_s$ , only depends on the topographic height of that point and does not vary with time. On the other hand, the computation of single-site pressure gradient for terrain slope with the pressure-based and terrain-following coordinate,  $\left(\frac{p - p_t}{p}\right) \cdot RT \cdot \nabla_s \ln(p_s - p_t)$ , depends on the accuracy of the computation of surface pressure and the vertical gradient of the hydrostatic pressure component.

### 3.2 Ideal experiments with the sensitivity of pressure gradient force computation to the surface pressure computation in the mass coordinates

From the analysis above, it is known that the two coordinates differ mainly in the coordinate slope, or, how the metric term is computed. For this reason, an ideal atmospheric experiment is designed to test the sensitivity of pressure gradient force computation in steep terrain to the computation of surface pressure.

The reference atmosphere used is expressed as

$$\begin{cases} \frac{\partial \bar{F}}{\partial \ln p} = -R\bar{T} \\ \left(-\frac{g}{C_p} + \frac{d\bar{T}}{dz}\right) \frac{R\bar{T}}{g} = C_0^2 \equiv \text{const} \end{cases} \quad (8)$$

where  $\bar{T}$  and  $\bar{F}$  are both the function of  $p$ . Taking the sigma coordinate as  $s = \frac{p}{p_s}$ , it is easy to prove that the horizontal pressure gradient force shows itself, in the reference atmosphere, on the sigma plane, as

$$\left(\frac{\partial \bar{F}}{\partial x(y)} + R\bar{T} \frac{\partial \ln p_s}{\partial x(y)}\right)_s = \nabla_p \bar{F} = 0 \quad (9)$$

During the ideal experiments, two kinds of terrain are available. One is an ideal sinusoidal terrain and the other actual model terrain (Fig.2a & b). The horizontal coordinate shows the number of gridpoints in the  $x$  direction and the vertical coordinate shows the height of the terrain in the unit of meter. The discrete expression (9) uses the centered difference format. During the experiments, it is found that the error of the difference for the pressure gradient force as derived with Eq.(9) will change when a bogus error is imposed on the surface pressure, especially where the terrain is steep. It justifies the argument that errors from the computation of surface pressure will result in those from the computation of the horizontal pressure gradient force. To see the difference more easily, the errors of the difference for the pressure gradient force with the bogus error is subtracted from those without the bogus error and the difference so obtained represents the errors in the computation of the pressure gradient force and the results are seen in Fig.2c. To further quantify the analysis of the sensitivity, the ideal sinusoidal terrain is replaced with model

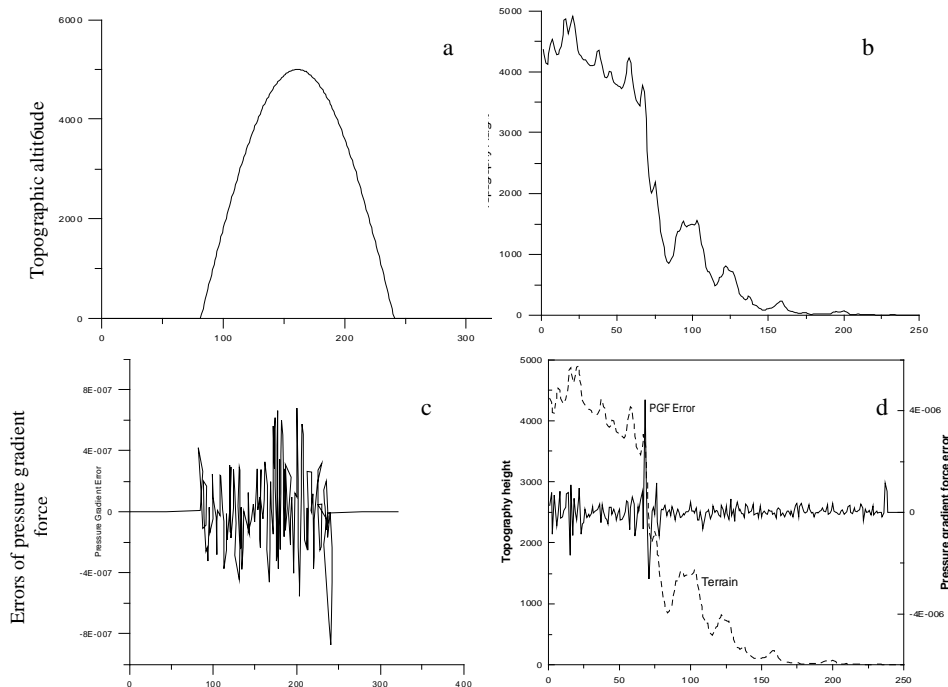


Fig.2 The cross-section of ideal terrain for the experiments and the errors of gradient force. (a) and (b) are the terrain taken in the ideal experiments and (c) and (d) are the errors of corresponding gradient force (the dashed lines indicate the terrain). Gridpoints are lined up horizontally.

terrain in actual weather forecasting (Fig.2) and with the same method, the difference between the two kinds of errors of difference is obtained and the result is used to construct Fig.2d. In the figure, the solid line is the difference for the plane where  $\sigma = 1.0$  by subtracting the pressure gradient force with the bogus error from those without the bogus error under the condition that the bogus error is equal to 1 hPa. It clearly shows that for the steepest places in plateau terrain (as indicated by the dashed line in Fig.2d), the error is the maximum for the pressure gradient force.

Horizontal pressure gradient force is an actual force. It should be the principle term of motion equations from the viewpoint of physics so that its magnitude has much influence on the nature of motion. The order of magnitude can be estimated from the following expression<sup>[12]</sup>

$$\frac{\partial p}{\partial x} \sim \frac{\partial p}{\partial y} \sim \frac{\Delta_h p}{L} \quad (10)$$

As shown by observation, the horizontal scale in the fronts on weather charts is  $L \sim 10^4$  m while the order of magnitude is  $10^0$  for the horizontal variation scale  $\Delta_h p$  of surface pressure. It is then clear that the order of magnitude should be  $10^{-4}$  for the horizontal pressure gradient force in mesoscale frontal systems. It is known from the experiment results that an error of 1 hPa in surface pressure on a  $\sigma = 1.0$  plane, or, the order of magnitude is  $10^{-6}$  for surface pressure gradient force, will bring about relative errors between 1% and 10%, 6% for places with steep terrain (Fig.2d). Likewise, the error of the pressure gradient force is at  $\sigma = 0.5$  plane, 4% relative error will also be resulted on steep terrain. The experiment results also show that the larger the bogus error of surface pressure, the larger the error it will lead to for the pressure gradient force.

It is therefore seen that the computation of pressure gradient force for steep terrain is sensitive to surface pressure. The accuracy directly governs the computed results of the horizontal wind field. Besides, the atmosphere, through horizontal convergence and divergence, affects the integration of vertical velocity, i.e. the accuracy of computed vertical velocity. It will be shown more clearly in the analysis of an actual case presented below.

## 4 CASE OF ACTUAL WEATHER — ANALYSIS OF VERTICAL VELOCITY AND FIELD OF RELATED ELEMENTS

### 4.1 Design of working experiments

#### 4.1.1 RESOLUTION, DYNAMIC FRAMEWORK AND PHYSICAL PROCESSES

The dynamic framework of the WRF model used in this work is a non-hydrostatic Euler dynamic one. For comparison, the height-based and terrain-following coordinate and pressure-based and terrain-following coordinate were both used. The Lambert projection was used for an area centered at  $35^\circ\text{N}$ ,  $110^\circ\text{E}$ . When model resolution takes 10 km, there are 251 gridpoints in both the meridional and zonal directions and the vertical is divided into 35 layers. The Runge-Kutta 3-order scheme is used for time integration, the NCEP 3-class simple ice scheme for the micro-physics, the Dudhia scheme for shortwave cumulus radiation physics, the Monin-Obukhov scheme for surface physics, a simple thermal dissipation scheme for surface processes, the MRF scheme for physical processes in the boundary layer, the Eta Kain-Fritsch shallow convection scheme as the cumulus solution. When model resolution is 30 km, all parameters remain the same except that there are no microphysics.

#### 4.1.2 INTRODUCTION TO THE DATASET

The NCEP analysis field is used as the initial field and the WRF model for its boundary condition. The NCEP dataset is the information about global mandatory isobaric layers issued in

the United States. The horizontal resolution is  $1^{\circ} \times 1^{\circ}$  and there are 26 vertical layers, the lowest being the 1000 hPa layer and highest 10 hPa.

#### 4.2 Analysis of actual experiment results

It is known from the above analysis that the two coordinates differ in the computation of pressure gradient force. For the pressure gradient at single points with the height-based and terrain-following coordinate, the computation of terrain slope does not rely on surface pressure but only on the terrain height of the model, and once the model terrain is acquired, the metric term on individual sigma planes remain unchanged; for the pressure gradient at single points with the pressure-based and terrain-following coordinate, the computation of terrain slope is done just the reversed way, for it not only depends on the computed pressure gradient on sigma planes but also the computed surface pressure for the metric term. As a result, any error or cumulated error on the part of surface pressure computations will distort the pressure gradient force derived, just as what the experiments have shown. In the meantime, it is important to note that the atmosphere is a continuous medium, in which any error of the horizontal wind field will act on the vertical motion of the whole atmosphere via divergence and convergence and influence the precipitation forecast eventually.

The case selected for the current work took place from 20:00(L.T.) June 7 to 02:00 June 10, 2002, which brought torrential rain to Xi'an and Han Zhong, in Shanxi province. The weather process was simulated using the dynamic framework of two different coordinates of the WRF model. During the forecast with the two models, all conditions remain unchanged, including the same physical processes, time integration schemes and spatial discrete schemes, number of vertical layers and horizontal resolution, except for different coordinates.

##### 4.2.1 TEMPORAL EVOLUTION OF SINGLE-POINT VERTICAL VELOCITY

To reflect the difference of vertical velocity under the same condition in different coordinates, the authors selected the temporal evolution of vertical velocity at a single point ( $33^{\circ}\text{N}$ ,  $107^{\circ}\text{E}$ ) with steep slope during the torrential rain in Shanxi province, with resolution at 10 km and 30 km. The main characteristics are shown in Fig.3. With resolution at 30 km and 10 km, respectively, the terrain of the WRF model is different. To clarify the issue, Fig.1a and 1b give the terrain profiles along  $33^{\circ}\text{N}$  with the two resolutions. Fig.1 shows that the terrain obtained with the 10-km resolution is much more detailed while that with the 30-km resolution much more smoothed out. Fig.3 shows that in either of the models, the variation of single-point vertical velocity with time looks similar in the vertical structure for the first 30-h forecast period. Then it differs much. The difference is mainly shown in the lower levels (900 hPa – 500 hPa) and higher levels (300 hPa – 150 hPa). With the 30-km resolution, the two models generally give much similar temporal variation of the vertical velocity at single points, only that the forecast center is larger and higher in height in the model of height-based and terrain-following coordinate.

Under the condition of high resolution, the difference in the vertical structure of the two models with the growth of model integration time is increasing. It is our view that the difference is caused by accumulated errors of computed pressure gradient force for steep terrain due to the difference in model terrain as acquired with different resolution. In other words, the terrain will be described in more details with high-resolution models than with low-resolution ones; for the same point in space, the topographic slope differs with terrain of different resolution, with the slope generally larger with high-resolution models than low-resolution models, leading to accumulated errors for pressure gradient force at steep terrain.



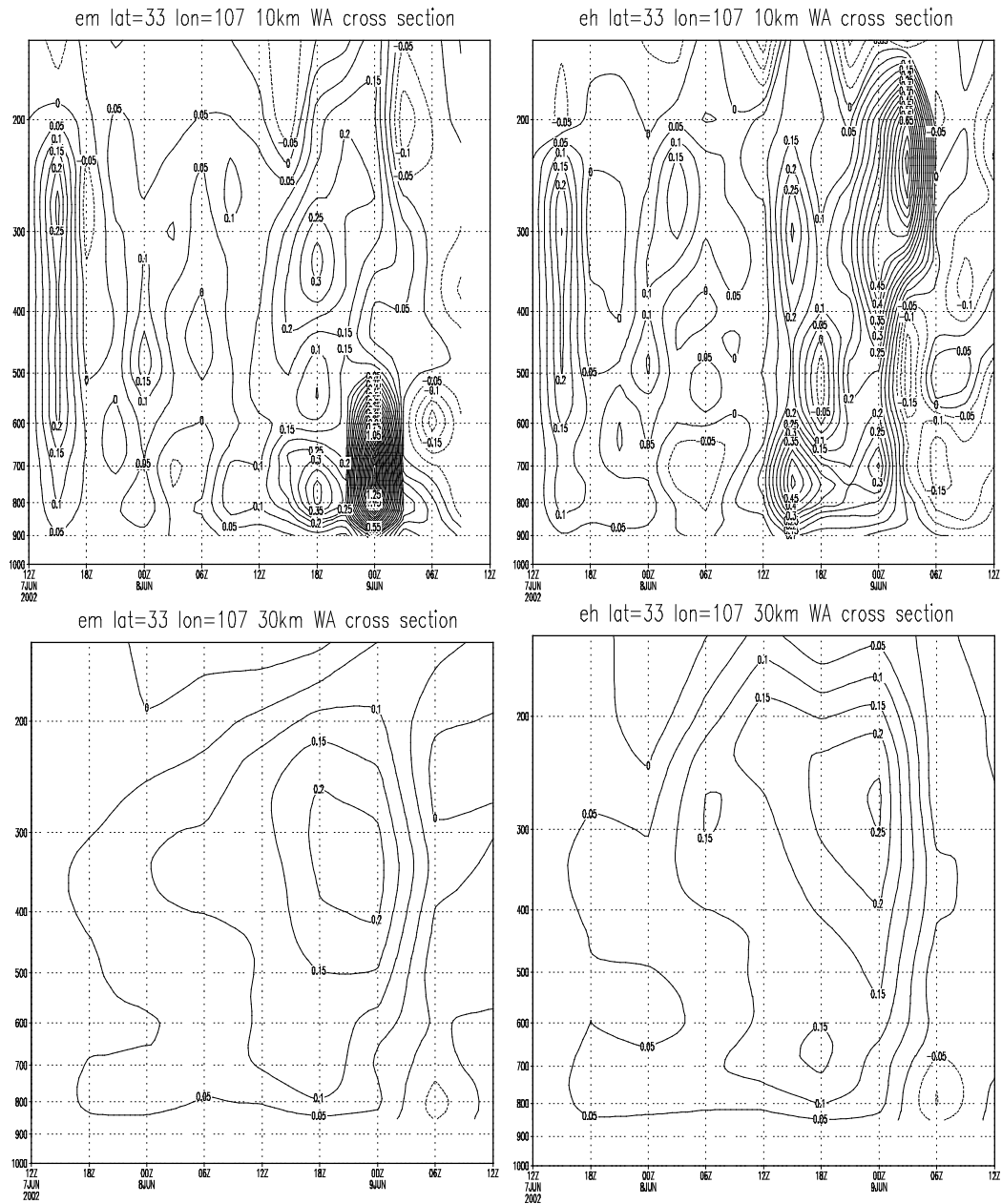


Fig.3 Temporal variation of the spatial single point (33°N, 107°E) with different resolution. (a) and (b) are the profiles of the mass and height coordinates with 10-km resolution and (c) and (d) the profiles with 30-km resolution.

#### 4.2.2 PROFILES OF SPATIAL VERTICAL VELOCITY

To further account for the general application of the vertical velocity differences as predicted with different coordinates under the same condition, the profiles of the spatial vertical velocity of the same torrential rain in Shanxi province is used. Similarly, profiles of vertical velocity are

analyzed along  $33^\circ\text{N}$ , with different resolutions.

Fig.4 shows that with moderate resolution (30 km), the structure of the vertical velocity does not differ much from each other, only that on levels of 300 – 200 hPa at  $110^\circ\text{E}$  the vertical

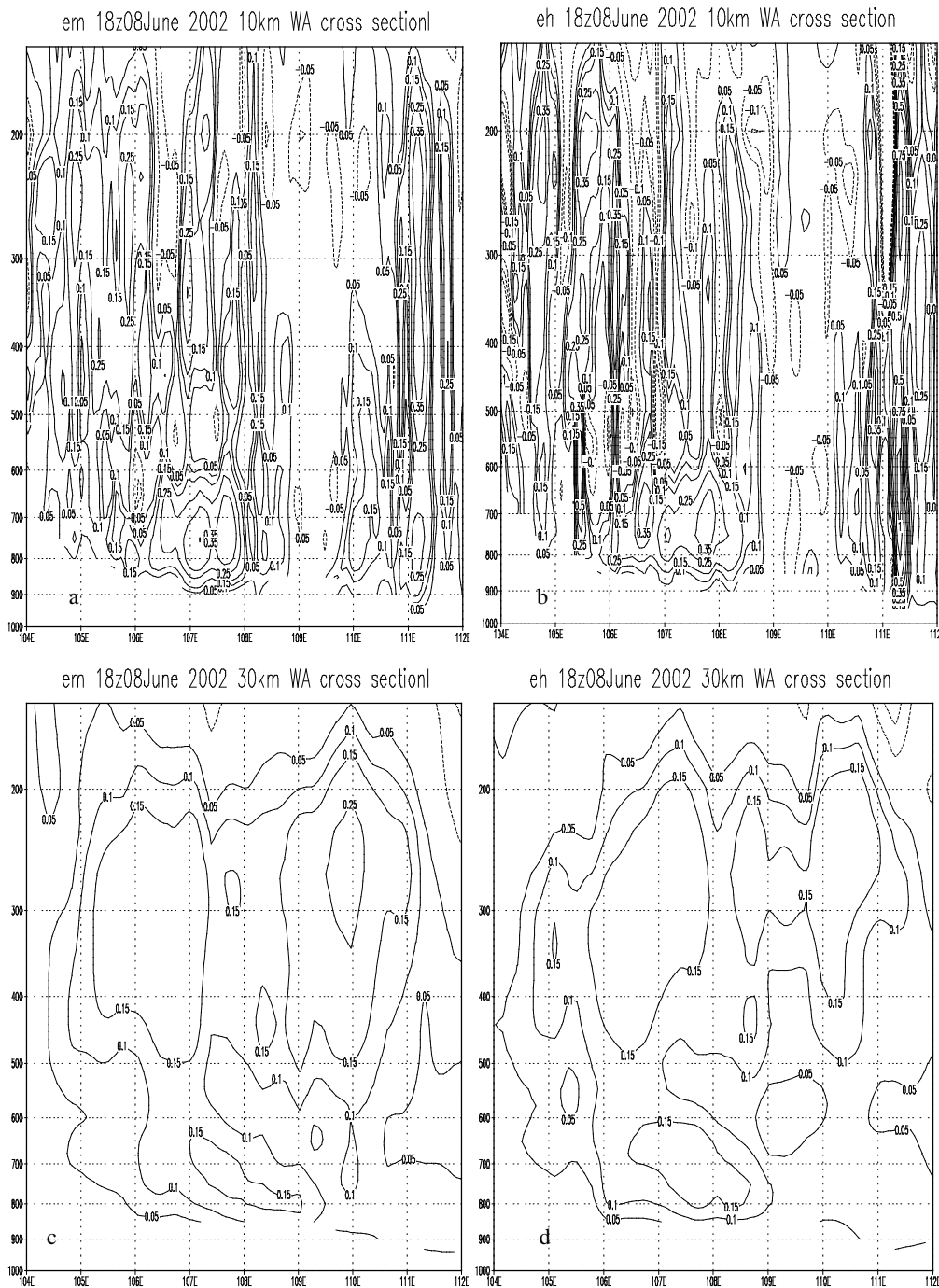


Fig.4 Profiles of vertical velocity along  $34^\circ\text{N}$  with the mass and height coordinates but different resolution. The captions are the same as Fig.3.

velocity is a little larger in the mass coordinate than that in the height coordinate. When resolution increases to 10 km, however, the vertical velocity predicted with the height coordinate is much larger than that with the mass coordinate, especially at 106°E and 111.3°E, respectively. Ascending motion is strong in the vertical direction at 106°E with the height coordinate but weak with the mass coordinate, in which weak descending motion occurs between 700 hPa and 600 hPa; ascending motion is much stronger at 111.3°E in both low and high levels of vertical direction with the height coordinate than with the mass coordinate.

It is known from the above theoretic analysis and results of ideal experiments that such difference in vertical velocity with all conditions but vertical coordinates remaining the same is caused by the fact that the terrain in the high-resolution models is relatively steep (Fig.1b) but relatively smooth in the low-resolution models (Fig.1a). For steep terrain, sensitivity of pressure gradient to the computation of surface pressure will result in the difference in the mass coordinate but won't do so in the height ordinate.

#### 4.2.3 SENSITIVITY EXPERIMENTS OF PRESSURE-BASED AND TERRAIN-FOLLOWING COORDINATE TO DISTURBANCE OF SURFACE PRESSURE

It is known from the above ideal experiments that the computed pressure gradient force is sensitive to surface pressure in the pressure-based and terrain-following coordinate. The computational errors of surface pressure will distort the values of pressure gradient force computed. It is also noted that the atmosphere is a continuous medium, in which any error of the horizontal wind field will act on the vertical motion of the whole atmosphere via divergence and convergence and influence the precipitation forecast eventually. In this work, a disturbance, which is 0.15% of the original surface pressure, is applied to the initial analysis field during the actual forecast of the weather case, to see whether it will affect the forecast results.

It is known from Fig.5 that the forecast results with initial disturbances differ from those without. It is much more clear from the field of 24-h vertical velocity (Fig.5a) and field of precipitation difference (Fig.5b): Places where the vertical velocity is the maximum (100°E, 111°E) are steep in terrain and places with the largest precipitation difference also witness strong precipitation.

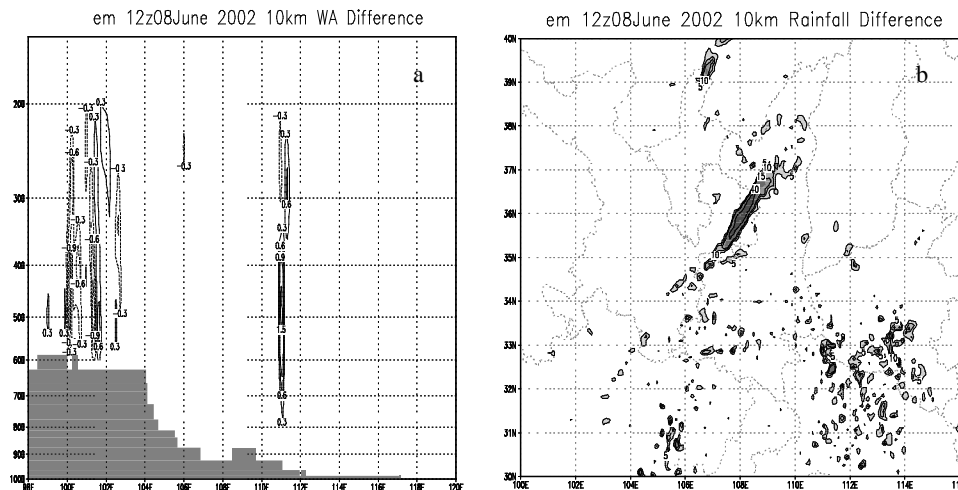


Fig.5 24-h forecast differences in the mass coordinate with and without initial surface pressure disturbance. a. Profiles of vertical velocity along 33°N in the 10-km resolution mass coordinate with and without initial disturbance (the shaded areas are terrain); b. Precipitation differences in the 10-km resolution mass coordinate with and without initial disturbance.

It can then be inferred that in the pressure-based and terrain-following coordinate, distorted surface pressure affects the accuracy of pressure gradient force computed for steep terrain and acts on the vertical motion of the whole atmosphere through convergence and divergence before influencing the actual weather forecasts.

## 5 CONCLUSIONS AND DISCUSSIONS

This work first devotes itself to studying of the difference between the mass coordinates and height coordinates and their relationship with the terrain. Then, on the basis of the analysis, it conducts ideal experiments on how the computation of pressure gradient force with the mass coordinates depends on the sensitivity of the computation of surface pressure. The results of actual weather forecasts are studied to compare the effects of individual coordinate on the computation of vertical structure in the actual atmosphere. From the theoretic analyses, ideal experiments and simulation of actual cases, the following preliminary conclusions can be drawn:

a. Theoretic analysis and ideal experiments have shown that the computation of pressure gradient force for steep terrain is sensitive to surface pressure; its accuracy will immediately affect the computation of horizontal wind field.

b. For a non-hydrostatic model, the computation of vertical velocity is linked with vertical coordinates and the computation of pressure gradient forces is also linked with vertical coordinates. As a result, pressure gradient force computed for different coordinate systems vary and lead to differences in the vertical velocity determined. The deviation is much associated with horizontal resolution.

c. In actual NWP models, when surface pressure is distorted with the pressure-based and terrain-following coordinates, it will cause errors in the computed vertical velocity in non-hydrostatic models and eventually affect the results of actual weather forecasts.

Effects of different coordinate systems on the computations of vertical velocity are only part of the effects of vertical coordinate systems. With the same conditions the other differences resulting from different vertical coordinate systems will be discussed elsewhere.

**Acknowledgements:** The authors would like to thank HUANG Li-ping, WU Xiang-jun, ZHANG Hong-liang, HU Jiang-lin, YANG Xue-sheng, JIN Zhi-yan, XU Guo-qiang at the CNPR (Center of Numerical Prediction Research) for their instruction on model run and other techniques. The authors would also like to thank JI Li-ren, CHEN Jia-bin, ZHANG Dao-ming and CHEN Xiong-shan for their invaluable opinions.

## REFERENCES:

- [1] Richardson L F. Weather prediction by numerical process [M]. New York: Cambridge University Press, 1965. 235.
- [2] ELIASSEN A. The quasi-static equations of motion with pressure as independent variable[J]. *Geofys Publikasjoner*, 1949, [J]. *Acta Oceanologica Sinica*, 1985, 7: 103-110.
- [3] CHEN Lie-ting. Effect of zonal difference of sea surface temperature anomalies in the Arabian Sea and the South China Sea on summer rainfall over the Yangtze River [J]. *Journal of Meteorology*, 1957, 14(2): 184-185.
- [4] SANGSTER W E. A method of representing the horizontal pressure force without reduction of station pressures to sea level[J]. *Journal of Meteorology*, 1960, 17(2): 166-176.
- [5] Gal-chen T, SOMERVILLE R C J. On use of a coordinate transformation for the resolution of the Navier-Stokes equation[J]. *J Comput Phys*, 1975, 17(2): 209-228.
- [6] MESINGER F. A blocking technique for representation of mountains in atmospheric models[J]. *Riv Meteor Aeronautica*, 1984, 44(2): 195-202.
- [7] RENE Laprise. The Euler equations of motion with hydrostatic pressure as an independent variable[J]. *Monthly Weather Review*, 1992, 12(2): 197-207.
- [8] ZHAO Ming. On the computation of the vertical velocity at the top of PBL in low latitude areas [J]. *Journal of Tropical Meteorology*, 1997, 13(1): 88-91.

- 
- [9] ARIRA Kasahara. various vertical coordinate systems used for numerical weather prediction[J]. *Monthly Weather Review*, 1974, **102**(5): 509-522.
- [10] LIAO Dong-xian, WANG Liang-ming. The Principles of NWP and Its Application [M]. Beijing: Meteorological Press, 1986. 29-31.
- [11] WANG Xing-bao, ZHANG Wei-huan. A numerical study of baroclinic disturbance excited by mountain ridge [J]. *Journal of Tropical Meteorology*, 1995, **11**(2): 150-161.
- [12] LU Mei-zhong, PENG Yong-qin. The Study Course of Dynamic Meteorology [M]. Beijing: Meteorological Press, 1990. 53-54.